ELSEVIER

Ceramics International 30 (2004) 447–452

CERAMICS INTERNATIONAL

www.elsevier.com/locate/ceramint

The magnetoresistance of $(Tb_{1-x}\ Sm_x)_{0.6}Sr_{0.4}MnO_{3+\gamma}$ manganites

Mihail-Liviu Craus[a,*], Nicoleta Cornei[b], Ioan Berdan[b], Carmen Mita[b], Mircea Nicolae Palamaru[b]

[a]*National Institute of Research & Development TPI Iasi, Blvd.D.Mangeron 47, 6600 Iasi, Romania*
[b]*"Al.I.Cuza" University, Chemistry Faculty, Blvd.Carol I, 6600 Iasi, Romania*

Received 27 March 2003; received in revised form 16 May 2003; accepted 6 June 2003

Abstract

$(Tb_{1-x}\ Sm_x)_{0.6}Sr_{0.4}MnO_{3\gamma}$ compounds were obtained by sol–gel method, by using oxides and acetates. The compounds were sintered in O_2 atmosphere at 1200 °C. The samples contain only a perovskite phase, with orthorhombic (Pnma) structure. Dependence of the tolerance factor and of the variance vs. chemical composition of the samples was observed. An increase of Tb concentration leads to a sudden decrease of the specific magnetization of the samples, but has little influence on the Curie temperature. A typical magnetoresistance behaviour (a maximum of the resistivity vs. T) was observed for the sample without Tb. The samples containing Tb have a decrease of the resistivity (ρ) vs. the intensity of the applied magnetic field and with the increase of the temperature ($d\rho/dT < 0$, typical for a semiconductor). An increase of the activation energy of the charge transport takes place with the increase of the Tb concentration in the samples.

Keywords: A. Sol–gel processes; B. X-ray methods; C. Electrical properties; C. Magnetic properties; D. Perovskites

1. Introduction

Manganite compounds of general formula $A_{1-x}B_xMnO_3$ (A is rare earth element, B is an alkaline earth metal) are of high technological importance because of their interesting electronic and magnetic properties, of their colossal magnetoresistance (CMR) and charge ordering properties [1–3]. The magnetoresistance effect can be described as a large decrease of the resistance on application of an external magnetic field and can be observed in some magnetic perovskites near the Curie temperature. "Colossal magnetoresistance" was first observed in multilayers or granular systems.

The colossal magnetoresistance, as a change of the resistivity vs. the applied magnetic field could be due to:

1. the melting of the long-range charge/orbital-ordered ground state [4];
2. a change in the relative fraction of a ferromagnetic (metallic) phase and insulating long-range charge/orbital-ordered domains [5];
3. a charge localization within the nanoferromagnetic cloud [6].

The conduction in $LnMnO_3$ like perovskites can be explained by supposing that the real fast charge transfer takes place via the equilibrium reaction [5]:

$$Mn(III)\left(t^3e^1\right) - O2p_\sigma^2 - Mn(IV)\left(t^3e^0\right) \quad (1)$$

where an electron from Mn(III) replaces the electron with the same spin from the oxygen on the free orbital e of the Mn(IV). It leads to a ferromagnetic order of magnetic moments associated with Mn cations.

Zener postulated also that below Curie temperature (T_C) the mobility of the cluster formed by two Mn cations is given by the equation [5]:

$$\mu = \frac{eD_0}{kT} \quad (2)$$

where e is electron charge, D_0 is the temperature-independent diffusion coefficient, k is the Boltzmann constant, T is the temperature. It leads to a linear dependence of the resistivity vs. temperature.

* Corresponding author. Tel.: +0232-130680.
E-mail address: craus@phys-iasi.ro (M.-Liviu Craus).

0272-8842/$30.00
doi:10.1016/S0272-8842(03)00130-5

In the manganese oxides stationary clusters grow with the decrease of the temperature, as the mobile species are progressively condensed into more conductive ferromagnetic clusters. The CMR occurs because the volume of these clusters grows also with the intensity of the applied magnetic field [7]. The $Sm_{0.55}Sr_{0.45}MnO_3$ samples were investigated by small-angle neutron scattering (SANS), the scattering results indicating the presence of the ferromagnetic clusters also in the paramagnetic phase [8].

In the presence of Mn^{3+} cations appears a strong coupling between the charge and the lattice and the Jahn–Teller distortions lift the degeneracy of e_g orbitals and can localize the corresponding electrons in the paramagnetic state. On other hand the increase of the e_g band quenches the Jahn–Teller distortions and delocalises the e_g electrons [8].

One of the most typical examples of the presence of the double-exchange is the $La_{1-x}Sr_xMnO_3$ system. The magnetic and electric behaviour near the Curie temperature can be explained by means of the electronic structure of the magnetic perovskites [9]. The FMR study of the manganite films [$(La, Nd)_x(Ca, Sr, Ba)_{1-x}MnO_{3+\gamma}$] indicated an inhomogeneous state of the samples containing high conductive regions (10^{-2} Ω.cm) and low-conductive regions (>1 Ω. cm) [10]. The $La_{1-x}Sr_xMnO_3$ [$x \in (0.25-0.5)$] compounds are fully ferromagnetic, Curie temperature being practically independent on Sr concentration in the sample [11].

It is known that at a low carrier density the ferromagnetic metallic regions can be seen as isolated droplets in an insulator antiferromagnetic matrix [12]. The increase of the electronic density leads to an increase of the ferromagnetic metallic regions and finally to the percolation of the ferromagnetic ordering in the crystal [12].

The purpose of present paper is to study the influence of the concentration ratio of Sm and Tb on the structure, magnetic and electric properties, including magnetoresistance, at some $(Tb_{1-x}Sm_x)_{0.6}Sr_{0.4}MnO_3$ compounds.

2. Experimental

The samples with the chemical composition $(Tb_{1-x}Sm_x)_{0.6}Sr_{0.4}MnO_3$, where $x=(0.45–1.0)$, were prepared by means of sol–gel method, using as precursors rare earth oxides (Tb_4O_7 and Sm_2O_3) (purity: 99.99%) and Sr and Mn acetates (purity: 99.00%). The oxides and the acetates were firstly solved in an aqueous solution of nitric acid and in an aqueous solution of acetic acid, respectively [13,14]. Then the precursors were mixed in corresponding stoechiometric ratios and a gel was obtained by addition of the aqueous solution of the citric acid (10%). The gel was heated at 105 °C to remove the excess of the solvent and calcinated at 300 °C to decompose the organic constituents.

The resulting powders were ground and pressed into pellets and presintered at 700 °C for 15 h in air. The presintered samples were again ground and finally sintered at 1200 °C for 7.5 h in O_2 atmosphere. The Mn^{4+} concentration was determined by an iodometric titration, by using sodium thiosulphate [15].

Phase composition, structure, lattice constants and volume of the lattice cell were monitorized by X-ray analysis in presintered and sintered samples. We used a diffractometer, equipped with a Co X-ray tube and previewed the results with a data acquisition system. The interplanar distances were corrected for the zero goniometer and the off set of the sample against the goniometer axis. The precision of the interplanar distances was better as 0.001 Å.

The electrical measurements were carried out using the four probes method between 77 and 450 K. The magnetic measurements were performed with a vibrating sample magnetometer between 77 and 600 K. The measuring system of the magnetoresistance and the magnetometer were also previewed with a data acquisition system.

3. Results and discussion

The structure of the sintered samples depends on the nature and the concentration of the rare earth cations. The samples contain only a phase, which has an orthorhombic structure—SG 62—Pmna (see Fig. 1) in agreement with the literature [14,16].

The volume of the unit cell of $Sm_{0.6}Sr_{0.4}MnO_{3+\gamma}$ is 224.55 Å^3, in agreement with the unit cell of $SrMnO_{2.69}$. This is thought to be due to the substitution of the Sr ($r_{Sr}=1.38$ Å) with a cation, which has a smaller radius ($r_{Sm}=1.098$ Å).

The volume of the unit cell has a minimum with the increase of the terbium concentrations in the $(Tb_{1-x}Sm_x)_{0.6}Sr_{0.4}MnO_{3+\gamma}$ samples (Table 1).

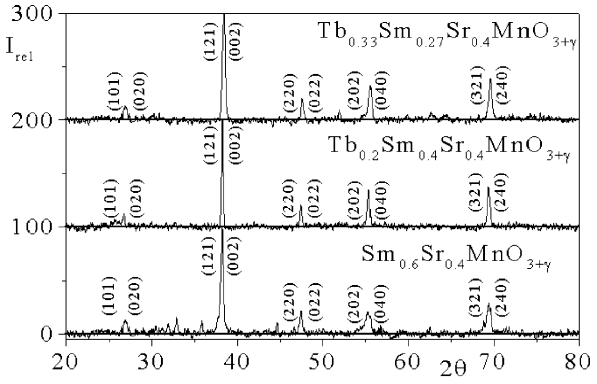

Fig. 1. The diffractograms of the $(Tb_{1-x}Sm_x)_{0.6}Sr_{0.4}MnO_{3+\gamma}$.

Table 1
The variation of the lattice constants vs. chemical composition

Chemical composition	a(Å)	b(Å)	c(Å)	V(Å^3)
$Sm_{0.6}Sr_{0.4}MnO_{3+\gamma}$	5.371	7.666	5.454	224.55
$Tb_{0.2}Sm_{0.4}Sr_{0.4}MnO_{3+\gamma}$	5.385	7.639	5.390	221.72
$Tb_{0.33}Sm_{0.27}Sr_{0.4}MnO_{3+\gamma}$	5.405	7.495	5.479	222.00

This could be due to: (1) the radii of Tb cations, which are smaller than the radii of Sm cations, (2) the increase of the cation vacancies concentration and (3) the decrease of the valence state of the Mn. The substitution of Sr with Sm, a cation with a radius smaller as that of Sr, leads to a decrease of the unit cell and also to a chemical disorder.

The decrease of the concentration of the cation vacancies is associated with the decrease of the tolerance factor (see Table 2) [17]:

$$t = \frac{d_{A-O}}{\sqrt{2}d_{M-O}} \quad (3)$$

where: d_{A-O} and d_{M-O} represent, respectively, the distance between the A (twelve fold O-coordinated) and O, respective, M (six fold O-coordinated) and O.

A strong dependence has been observed of the variance σ^2, defined by equation $\sigma^2 = \Sigma y_i r_i^2 - r_A^2$ (r_i represent the radii of the rare earth cations and of the Sr cation, r_A is the average radius of the A placed cation and y_i is their occupancies of the i ions, $\Sigma y_i = 1$) on the chemical composition (see Table 2).

The increase of Tb concentration in the $(Tb_{1-x}Sm_x)_{0.6}Sr_{0.4}MnO_{3+\gamma}$ compounds seems to lead to a decrease of the Mn^{3+} and Mn^{4+} concentration ratio. The decrease of the Mn^{3+} and Tb^{3+} concentration in the sample is associated with the increase of the degree of the chemical disorder and a decrease of the tolerance factor (see Table 2).

Concerning the magnetic properties of the $(Tb_{1-x}Sm_x)_{0.6}Sr_{0.4}MnO_{3+\gamma}$ samples, we observed that the magnetic moment per molecule sudden decreases vs. increase of Tb concentration: the specific magnetization decreases about five times by substitution of 0.2 Sm atoms with an equivalent Tb quantity (see Table 2 and Fig. 2). The double exchange interaction between the Mn^{3+} and Mn^{4+} is responsible for the total magnetic moment of the sample. The specific magnetization at low temperatures is practically independent of the temperature and decreases with an increase of Tb concentration in the sample, although the magnetic moment of Tb is much greater than that of Sm. On other hand, the magnetic moment of the studied perovskites is smaller than the one due to a ferromagnetic alignment of the magnetic moment of Mn.

The magnetic coupling between the neighbour manganese cations is due to an overlap of a strong double exchange interaction and a weak super-exchange interaction. The double exchange interaction leads to the appearance of a ferromagnetic state (parallel alignment of elementary magnetic moments), while the super-exchange interaction enhances the antiferromagnetic alignment of the magnetic moments. Because Mn^{4+} concentration increases with the increase of Tb concentration in the perovskites with $(Tb_{1-x}Sm_x)_{0.6}Sr_{0.4}MnO_{3+\gamma}$ (see Table 3) composition, the result is an increase of the super-exchange interaction relative to the double exchange interaction. The double exchange interaction remains dominant for the samples with a Tb concentration less or equal with 0.2, but decrease with the increase of the Tb concentration.

The decrease of the specific magnetisation vs. the increase of Tb concentration could be due to the following factors:

- To the increase of the chemical disorder, which leads to the decrease of the molecular field intensity and consequently determines the orientation of magnetic moments associated to the manganese cations. In a simple model, the magnetic moments of Mn cations are randomly distributed on a conic surface. The increase of the magnetic field could lead to an increase of the total magnetic moment of the sample. On other hand, the increase of the disorder degree leads to an increase of the average angle between the atomic magnetic moments and implicitly to a lowering of the total magnetic moment of the sample. The increase of the chemical disorder enhances the fluctuation degree of the length and of the angle of the Mn–O–Mn bonds, these parameters being very important for the double exchange interaction [20].

Table 2
The variation of the Curie temperature (T_C), concentration of Mn^{3+}–Mn^{4+} couples ($C_{Mn3+-Mn4+}$), tolerance factor (t), the chemical disorder (σ^2) and magnetic moments of the molecule (p)

Chemical composition	T_C (K)	$C_{Mn3+-Mn4+}$	t	σ^2(Å^2)	$p(\mu_B)$[a]
$Sm_{0.6}Sr_{0.4}MnO_{3+\gamma}$	192.2	0.30	0.941	0.866 10^{-2}	2.11
$Tb_{0.2}Sm_{0.4}Sr_{0.4}MnO_{3+\gamma}$	194.0	0.06	0.930	1.616 10^{-2}	0.43
$Tb_{0.33}Sm_{0.27}Sr_{0.4}MnO_{3+\gamma}$	191.8	0.015	0.924	2.087 10^{-2}	0.10

[a] The values calculated from the magnetic measurements accomplished at 77 K.

Table 3
The activation energy (E_a) of the transport properties of the $(Tb_{1-x}Sm_x)_{0.6}Sr_{0.4}MnO_{3+\gamma}$ samples and concentration Mn^{3+}/Mn^{4+}

Chemical composition	T(K)	E_a(eV)	γ	Concentration Mn^{3+}	Concentration Mn^{4+}
	$H=0$ T				
$Sm_{0.6}Sr_{0.4}MnO_{3+\gamma}$	130÷200	0.226	0.01	0.58	0.42
	200÷265	0.056			
$Tb_{0.2}Sm_{0.4}Sr_{0.4}MnO_{3+\gamma}$	125÷250	0.3	0.035	0.53	0.47
$Tb_{0.33}Sm_{0.27}Sr_{0.4}MnO_{3+\gamma}$	144÷263	0.363	0.048	0.5	0.5

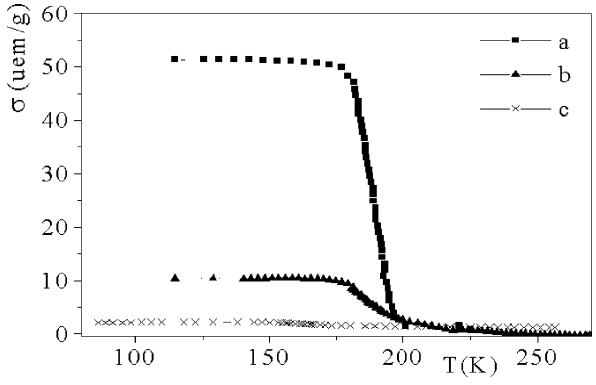

Fig. 2. The dependence of specific magnetization vs. chemical composition for the $(Tb_{1-x}Sm_x)_{0.6}Sr_{0.4}MnO_{3+\gamma}$ system trated in O2: (a) $Sm_{0.6}Sr_{0.4}MnO_{3+\gamma}$; (b) $Tb_{0.2}Sm_{0.6}Sr_{0.4}MnO_{3+\gamma}$; (c) $Tb_{0.33}Sm_{0.6}Sr_{0.4}MnO_{3+\gamma}$.

- To the fact that Tb does not participate to the exchange interaction and implicitly to the magnetic moment of the sample.
- To the concentration decrease of Mn^{3+}–Mn^{4+} couples (see Table 2).

According to Terai [21], the lower the tolerance factor the lower the Mn–O–Mn bond angles. This means that the interaction between the magnetic atoms decreases, or that there is a decrease of the magnetic atoms number, which contributes to the total magnetic moment of the sample. The increase of chemical disorder leads to the formation of regions where the magnetic moments of the Mn are parallel, separated by regions where the Mn magnetic moments are antiferromagnetically coupled. The presence of Tb seems to enhance the appearance of an antiferromagnetic insulator phase. The Curie temperature of the doped samples slightly decreases vs. Tb concentration (see Table 2). This happens even when Sm, which has a small magnetic moment (0.1 μ_B), is substituted with Tb (9.5 μ_B). The main ferromagnetic interaction takes place between the Mn cations and is practically independent relative to the distance between the Mn cations or to the substitution of Sr cations with rare earth cations.

The $Sm_{0.6}Sr_{0.4}MnO_{3.01}$ sample has a magnetoresistive effect, the transition temperature being about 125 K. In the temperature range where the measurements were performed, it was not observed a semiconductor to metallic state transition for the Tb containing samples (see Figs. 3 and 5). This behaviour is similar to that observed for other compounds as: $La_{1-x}Ca_xMnO_3$ (Wagner et al. [18]) and $Ho_{0.5}Sr_{0.5}MnO_3$ (Autret et al. [19]). According to the results obtained by Autret et al. [19], the substitution of Sm^{3+} with a smaller radius cation (e.g. the substitution of Sm with Tb) could lead to an increase of local microstrains, modifying the angle and the length of Mn–O–Mn bonds. On other hand, the colossal negative magnetoresistance (CMR) is correlated with the transition from the ferro- to the paramagnetic state and depends on the intensity of the magnetic field and on the tolerance factor in $Ln_{0.7}Ca_{0.3}MnO_{3+\gamma}$ system (Ln = rare earth or Y) [18].

Tb cation has a radius which is closer to the ideal radius of the A site comparing with the Ho radius, which means that the local microstrains of the lattice are smaller for $(Tb_{1-x}Sm_x)_{0.6}Sr_{0.4}MnO_{3+\gamma}$ as for $Ho_{0.5}Sr_{0.5}MnO_3$. This fact justifies a stronger dependence between the resistivity of $(Tb_{1-x}Sm_x)_{0.6}Sr_{0.4}MnO_{3+\gamma}$ samples and the magnetic field, comparing with $Ho_{0.5}Sr_{0.5}MnO_3$ [19].

The $(Tb_{1-x}Sm_x)_{0.6}Sr_{0.4}MnO_{3+\gamma}$ samples have different behaviours of the resistivity vs. Tb/Sm concentration ratio and temperature (see Figs. 3 and 4). The increase of the Tb concentration in the sample leads to an increase of the oxygen concentration (see Table 3). The decrease of the Mn^{3+}/Mn^{4+} ratio is associated

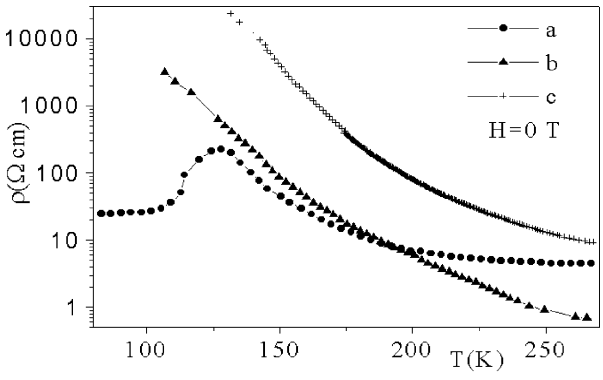

Fig. 3. The variation of the resistivity of the $(Tb_{1-x}Sm_x)_{0.6}Sr_{0.4}MnO_{3+\gamma}$ samples: (a) $Sm_{0.6}Sr_{0.4}MnO_{3+\gamma}$; (b) $Tb_{0.2}Sm_{0.6}Sr_{0.4}MnO_{3+\gamma}$; (c) $Tb_{0.33}Sm_{0.6}Sr_{0.4}MnO_{3+\gamma}$.

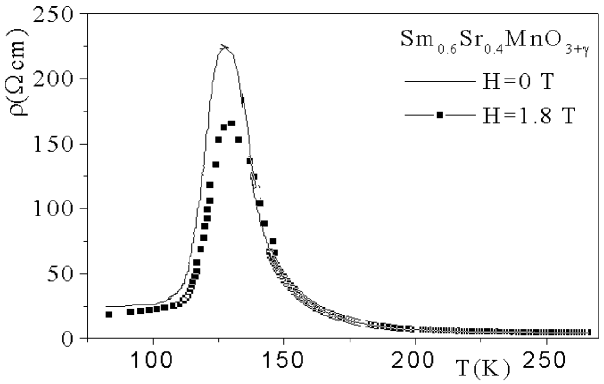

Fig. 4. The variation of the resistivity vs. temperature for $Sm_{0.6}Sr_{0.4}MnO_{3.01}$.

with a change in the resistivity behaviour (see Table 3 and Fig. 3).

For the $Sm_{0.6}Sr_{0.4}MnO_{3.01}$ oxide, we have observed a transition from metallic to semiconductor behaviour, in the investigated range of the temperatures, (see Fig. 4). This observation is in agreement with other authors' results [22].

For low magnetic fields and low temperatures, the absolute magnitude of the magnetoresistance for the $Sm_{0.6}Sr_{0.4}MnO_{3.01}$ sample is described by the following relation (see Fig. 4):

$$|MR| = \frac{A}{2T}bH \tag{4}$$

where A represents the height of energy barrier between two states of a ferron pair, MR is the standard definition of the magnetoresistance, H is the applied field, b is a constant which describes the antiferromagnetic exchange between local spins in neighbouring layers [23].

The samples behave as semiconductors for temperatures higher than the transition temperatures. The activation energy of the conduction becomes apparently smaller when a magnetic field is applied (see Fig. 5), indicating that the samples are magnetoresistive. The activation energy associated with the charge transport

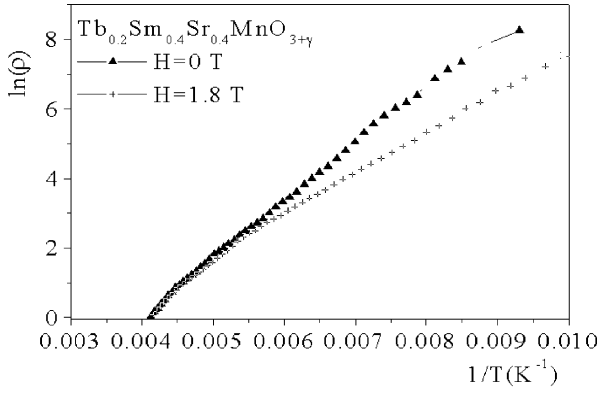

Fig. 5. The variation of the resistivity of the $Tb_{0.2}Sm_{0.4}Sr_{0.4}MnO_{3.035}$.

generally increases with the increase of the rare earth and Mn^{4+} concentrations. On other hand, when the activation energy is higher than 0.3 eV, the magnetoresistivity (corresponding to $Tb_{0.33}Sm_{0.27}Sr_{0.4}MnO_{3+\gamma}$) becomes zero.

4. Conclusions

The nature and the concentration of rare earth cations, which substituted Sr cations, determined the structure and the magnetoresistivity behaviour of the $(Tb_{1-x}Sm_x)_{0.6}Sr_{0.4}MnO_{3+\gamma}$ manganites. The substitution of Sm with Tb leads to changes of the unit cell parameters and to the modification of the magnetic cations interaction.

The increase of Tb concentration in the samples leads to the increase of the chemical disorder and, consequently, to an increase of the super-exchange interaction comparing with the double-exchange interaction. An increase of the average angle of Mn–O–Mn bonds takes place concomitantly with a diminishing of the magnetic moment of the sample. For the samples with Tb concentration higher than 0.2 the samples behave as an antiferromagnet.

If we corroborate the resistivity variation vs. temperature for different Tb concentrations, alternatively measured in the absence and in the presence of the magnetic field, we can conclude that for Tb concentrations higher than 0.33/chemical formulas the magnetoresistive effect disappears.

The substitution of Sm with Tb cations could led to a displacement of transition temperature from metallic to semiconductor state at lower temperatures, including a possible cancellation of the metallic state, for relatively high values of Tb concentration in the sample.

References

[1] W. Boujelben, A. Cheikh-Rouhou, J. Pierre, J.C. Joubert, J. Alloys Compounds 314 (2001) 15–21.
[2] J. Fontcuberta, B. Martinez, A. Seffar, S. Pinol, J.L. Garcia-Munoz, X. Obradors, Phys. Rev. Lett. 76 (7) (1996) 1122–1125.
[3] C. Martin, A. Maignan, M. Hervieu, B. Raveau, J. Jirák, A. Kurbakov, V. Trounov, G. André, F. Bourée, J. Magn. Magn. Mater. 205 (1999) 184–198.
[4] A. Urushibara, Y. Moritomo, T. Arima, A. Asamitsu, G. Kido, Y. Tokura, Phys. Rev. B 51 (1995) 14103–14109.
[5] C. Zener, Phys. Rev. 82 (1951) 440–447.
[6] P.W. Anderson, H. Hasegawa, Phys. Rev. 100 (1955) 675–681.
[7] J.B. Goodenough, Annual Rev. Mater. Sci. 28 (1998) 1–27.
[8] M. Quijada, J. Cerne, J.R. Simpson, H.D. Drew, K.H. Ahn, A.J. Millis, R. Shreekala, R. Ramesh, M. Rajeswari, T. Venkatesan, Phys. Rev. B 58 (1998) 16093–16102.
[9] Y. Tokura, Y. Tomioka, J. Magn. Magn. Mater. 200 (1999) 1–23.
[10] R. Ramesh, Annual Conference Magnetism and Magnetic Materials, Abstracts (1995) 196.
[11] G. Matsumoto, IBM J. Res. Develop 14 (1970) 258–260.

[12] E.L. Nagaev, Usp. Fiz. Nauk 39 (1996) 781–805.
[13] J.H. Kuo, H.U. Anderson, J. Solid State Chem. 87 (1990) 55–63.
[14] J. Mizusaki, H. Tagawa, Solid State Ionics 49 (1991) 111–118.
[15] J. Philip, T.R.N. Kutty, Mater. Chem. Phys. 63 (2000) 218–225.
[16] J. Töpfer, J.P. Doumerc, J.C. Grenier, J. Mater. Chem. 6 (1996) 1511–1516.
[17] J.B. Goodenough, J. Appl. Phys. 81 (8) (1997) 5330–5335.
[18] P. Wagner, I. Gordon, A. Das, J. Vanacken, V.V. Moshchalkov, Y. Bruynseraede, Int. J. Mod. Phys. B 14 (2000) 3735–3740.
[19] C. Autret, C. Martin, A. Magnan, A. Hervieu, B. Raveau, J. Solid State Chem. 165 (2002) 65–73.
[20] K. Liu, X.W. Wu, K.I. Ahn, T. Sulechek, C.L. Chich, J.Q. Xiao, Phys. Rev. B 54 (1996) 3007–3010.
[21] T. Terai, T. Sasaki, T. Kakeshita, T. Fukuda, T. Saburi, H. Kitagawa, K. Kindo, M. Honda, Phys. Rev. 61 (2001) 3488–3493.
[22] P.H. Wagner, V. Metlushko, L. Trappeniers, A. Vantomme, J. Vanaken, G. Kido, V.V. Moshchalkov, Y. Bruynseraede, Phys. Rev. B 55 (1997) 3699–3707.
[23] M. Yu Kagan, K.I. Kugel, Uspekhi Fizicheskikh Nauk 44 (2001) 553–570.